

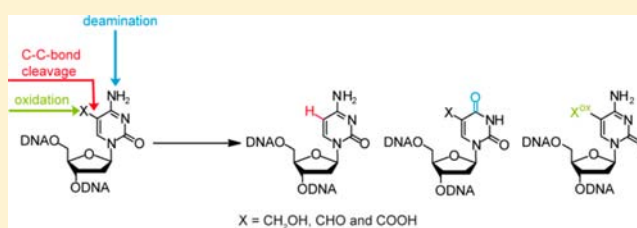
# Deamination, Oxidation, and C–C Bond Cleavage Reactivity of 5-Hydroxymethylcytosine, 5-Formylcytosine, and 5-Carboxycytosine

Stefan Schiesser,<sup>†,‡</sup> Toni Pfaffeneder,<sup>†,‡</sup> Keyarash Sadeghian,<sup>†,‡</sup> Benjamin Hackner,<sup>†</sup> Barbara Steigenberger,<sup>†</sup> Arne S. Schröder,<sup>†</sup> Jessica Steinbacher,<sup>†</sup> Gengo Kashiwazaki,<sup>†</sup> Georg Höfner,<sup>§</sup> Klaus T. Wanner,<sup>§</sup> Christian Ochsenfeld,<sup>†,‡</sup> and Thomas Carell<sup>\*,†</sup>

<sup>†</sup>Center for Integrated Protein Science (CiPS<sup>M</sup>) at the Department of Chemistry, <sup>‡</sup>Chair for Theoretical Chemistry at the Department of Chemistry, <sup>§</sup>Center for Drug Research at the Department of Pharmacy, Ludwig-Maximilians-Universität München, Butenandtstrasse 5-13, 81377 Munich, Germany

## Supporting Information

**ABSTRACT:** Three new cytosine derived DNA modifications, 5-hydroxymethyl-2'-deoxycytidine (hmdC), 5-formyl-2'-deoxycytidine (fdC) and 5-carboxy-2'-deoxycytidine (cadC) were recently discovered in mammalian DNA, particularly in stem cell DNA. Their function is currently not clear, but it is assumed that in stem cells they might be intermediates of an active demethylation process. This process may involve base excision repair, C–C bond cleaving reactions or deamination of hmdC to 5-hydroxymethyl-2'-deoxyuridine (hmdU). Here we report chemical studies that enlighten the chemical reactivity of the new cytosine nucleobases. We investigated their sensitivity toward oxidation and deamination and we studied the C–C bond cleaving reactivity of hmdC, fdC, and cadC in the absence and presence of thiols as biologically relevant (organo)catalysts. We show that hmdC is in comparison to mdC rapidly oxidized to fdC already in the presence of air. In contrast, deamination reactions were found to occur only to a minor extent. The C–C bond cleavage reactions require the presence of high concentration of thiols and are acid catalyzed. While hmdC dehydroxymethylates very slowly, fdC and especially cadC react considerably faster to dC. Thiols are active site residues in many DNA modifying enzymes indicating that such enzymes could play a role in an alternative active DNA demethylation mechanism via deformylation of fdC or decarboxylation of cadC. Quantum-chemical calculations support the catalytic influence of a thiol on the C–C bond cleavage.

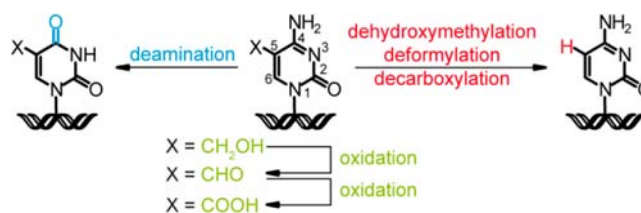


## INTRODUCTION

In addition to the canonical nucleosides dA, dC, dG, and dT, mammalian DNA contains 5-methyl-2'-deoxycytidine (mdC) and further dC derivatives that are generated from mdC by oxidation of the methyl group. The oxidizing enzymes are TET (ten eleven translocation) enzymes. These are  $\alpha$ -ketoglutarate dependent oxygenases, which oxidize 5-methyl-2'-deoxycytidine to 5-hydroxymethyl-2'-deoxycytidine (hmdC) and further to 5-formyl-2'-deoxycytidine (fdC) and 5-carboxy-2'-deoxycytidine (cadC).<sup>1–5</sup> The fate of these nucleosides and their function are currently controversially discussed. For hmdC for example it was postulated that the nucleoside may be deaminated *in vivo* to give 5-hydroxymethyl-2'-deoxyuridine (hmdU) by the action of special deaminases such as the AID (activation-induced deaminase)/APOBEC (apolipoprotein B mRNA-editing enzyme complex) protein family.<sup>6,7</sup> However, newer *in vitro* data suggest that deamination of hmdC is unlikely to occur enzymatically,<sup>8</sup> raising the question of whether the occurrence of hmdU may result from non-enzymatic spontaneous deamination of hmdC. Furthermore, since hmdC and fdC are known oxidative lesions of mdC<sup>9–11</sup> and because the levels of fdC and in particular cadC<sup>3–5,12</sup> are in the range of those reported for 8-oxo-dG,<sup>13</sup> which is a well-

known oxidative damage, one has to consider the possibility that they are formed by nonenzymatic oxidation processes

### Scheme 1. The dC Derivatives hmdC, fdC, and cadC Could Either Deaminate to dU Derivatives (Left), Undergo C–C bond Cleavage to dC (Right), or Oxidize



during DNA isolation and analysis.<sup>13,14</sup> Finally, while there is a possibility that enzymatic dehydroxymethylation of hmdC, deformylation of fdC, and decarboxylation of cadC might occur,<sup>15–19</sup> it cannot be ruled out that these processes occur

Received: April 11, 2013

Published: August 27, 2013

already to a significant extent without the help of an enzyme.<sup>18,20</sup>

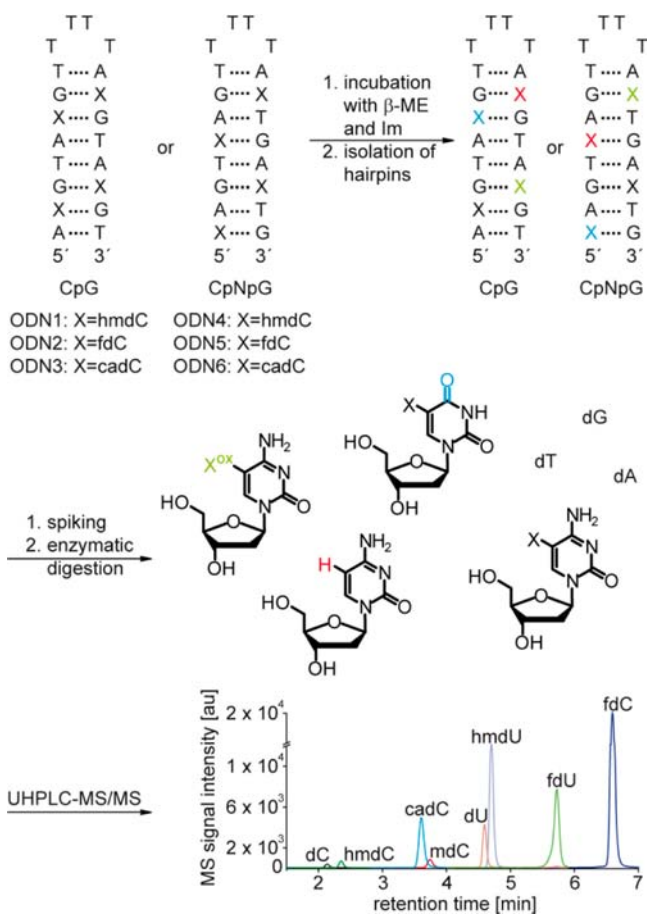
To differentiate between potential nonenzymatic background reactivities and enzyme-catalyzed processes, it is therefore essential to understand the intrinsic reactivity profile of the new nucleosides hmdC, fdC and cadC (Scheme 1).

## RESULTS AND DISCUSSION

Recently, others and us reported the synthesis of phosphoramidite and triphosphate building blocks for hmdC, fdC, and cadC and their incorporation into oligonucleotides using either solid phase phosphoramidite chemistry or by polymerase chain reaction (PCR).<sup>21–25</sup> For this study we synthesized hmdC, fdC, and cadC nucleosides and phosphoramidites and incorporated the latter into 20mer hairpin-oligodeoxynucleotides (ODN) with either hmdC (ODN1 and ODN4), fdC (ODN2 and ODN5), or cadC (ODN3 and ODN6) in a double-stranded xCpG or xCpNpG context using solid phase phosphoramidite chemistry (Scheme 2).

To investigate deamination-, oxidation-, and C–C bond cleavage reactions, the reactivities of the new epigenetic modifications were studied on the nucleoside level and in

**Scheme 2. Depiction of the Hairpins Used in This Study and of the Experimental Workflow<sup>a</sup>**



<sup>a</sup>After incubation of the xC-containing hairpins in  $\beta$ -mercaptoethanol ( $\beta$ -ME)/imidazole, the DNA was isolated. The corresponding isotopologues were added (omitted for clarity in the chromatogram), and the DNA was digested. Quantification of the reaction products was performed by UHPLC-MS/MS. Im = imidazole.

hairpin ODNs in buffer and in the presence of thiols. We investigated the reactivity with thiols in order to simulate potential enzymatic reactions, which often start by initial nucleophilic attack of the thiol at the C6 position of the pyrimidine. This then activates the corresponding C5 position (numbering see Scheme 1).<sup>18</sup> Examples are the DNA methyltransferases (DNMT), which convert dC to mdC.<sup>19</sup>

We first studied the reactivity of the different xC-nucleosides at pH 7.4 in buffer at different temperatures. We simultaneously quantified the various oxidation, deamination, and C–C bond cleavage reactions. Moreover, to elucidate how thiol-mediated C5 activation would influence the reactions, we performed studies with a systematic increase of  $\beta$ -mercaptoethanol ( $\beta$ -ME, 0 to 12 M). High thiol concentrations (12 M) were chosen to simulate the high effective molarity of, for example, the reactive cysteine moiety in the active sites of enzymes.<sup>17,18</sup> In all cases we performed product analysis using a UHPLC-MS/MS method with a triple quadrupole mass spectrometer (Scheme 2; for method development see Supporting Information [SI]). The developed method allows sensitive and accurate quantification of the whole product spectrum in one single analysis (12 min total run time). The exact quantification of the reaction products was conducted using the stable isotope dilution technique as described by others and us.<sup>12,13,26,27</sup> For the synthesis of the used isotopologues [<sup>15</sup>N<sub>2</sub>]-dC, [D<sub>2</sub>,<sup>15</sup>N<sub>2</sub>]-hmdC, [<sup>15</sup>N<sub>2</sub>]-fdC, [<sup>15</sup>N<sub>2</sub>]-cadC, [D<sub>3</sub>]-dT, [<sup>15</sup>N<sub>2</sub>]-dU, [D<sub>2</sub>]-hmdU, and [<sup>15</sup>N<sub>2</sub>]-fdU see SI.

**Oxidation Processes.** Our first question was how quickly air would oxidize mdC to hmdC, hmdC to fdC, and fdC to cadC. We dissolved the respective nucleosides in a phosphate buffer at pH = 7.4 and incubated the solution exposed to air for up to 60 h at 60.0, 67.5, 75.0, and 80.0 °C (Figure 1 and SI).

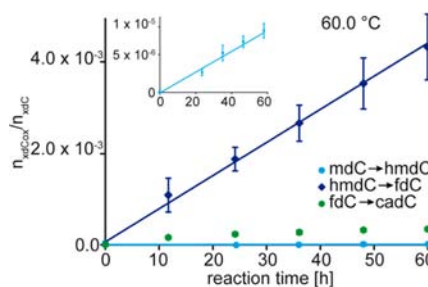


**Figure 1.** Oxidation kinetics of mdC to hmdC (cyan), hmdC to fdC (blue), and fdC to cadC (green) at 60.0 °C at pH 7.4. While hmdC is efficiently oxidized to fdC, fdC gives only a little cadC. Depicted are the means of triplicate experiments; error bars reflect the standard deviations. For details of the kinetic measurements at 67.5, 75.0, and 80.0 °C and linear regression analyses see SI.

For data analysis we assumed a pseudo-first order kinetic profile in which the oxygen concentration is a not rate limiting factor. Under these conditions we observed that mdC is oxidized only to a small extent to hmdC. In contrast, hmdC reacts efficiently to form fdC (Figure 1, blue line). Oxidation of fdC to cadC (Figure 1, green dots) is slow.

After 60 h at 60 °C, the yield of cadC was only 0.03%. Table 1 summarizes the determined pseudo-first-order rate constants. The data show that the formation of fdC by oxidation of hmdC is more than 2 orders of magnitude faster than the oxidation of mdC to hmdC. For the fdC to cadC oxidation, a rate constant

**Table 1.** Rate Constants  $k$  for the Oxidation of mdC to hmdC and hmdC to fdC at pH 7.4. For the Rate Constants at Higher Temperatures see SI<sup>a</sup>

	$k_{37\text{ }^\circ\text{C}}$ [ $\text{s}^{-1}$ ]	$k_{60\text{ }^\circ\text{C}}$ [ $\text{s}^{-1}$ ]	$E_a$ [ $\text{kJ mol}^{-1}$ ]
mdC→hmdC	n.d.	$4.7 \pm 0.6 \times 10^{-11}$	n.d.
hmdC→fdC	$1.3 \pm 0.1 \times 10^{-8}$	$2.2 \pm 0.2 \times 10^{-8}$	$20.8 \pm 2.2$

<sup>a</sup>n.d. = not determined.

could not be calculated, since the data deviated substantially from linearity (see Figure 1 and SI, Figure S2, Figure S11).

We next studied the oxidation reactions of hmdC and fdC in the hairpin-ODNs (Scheme 2). The reactions were performed without and with increasing amounts of  $\beta$ -ME (and imidazole at pH 5.0) in solution for 48 h at 50 °C (melting temperatures of hairpins:  $\geq 70$  °C; see SI, Table S1). The samples were desalted with a 0.025  $\mu\text{m}$  filter, spiked with the labeled internal standards, then fully digested with nuclease S1, snake venom phosphodiesterase, and antarctic phosphatase and analyzed by LC-MS/MS (Scheme 2). The amounts of the nucleoside products were normalized to the amount of dT [%]. Despite the shielding effect of the duplex environment, which could limit the reaction of the thiol at the C6 position, we measured increasing amounts of fdC with increasing concentrations of  $\beta$ -ME in ODN1 (hmdC). The fdC compound reached surprisingly high levels of up to 20% at 12 M  $\beta$ -ME (80% v/v  $\beta$ -ME; Figure 2, blue curve), showing that the C5–C6

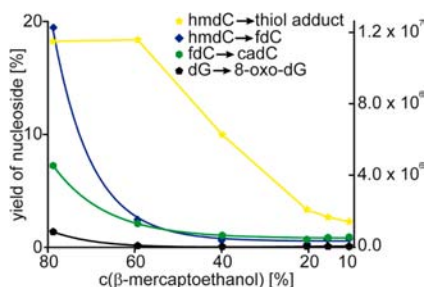


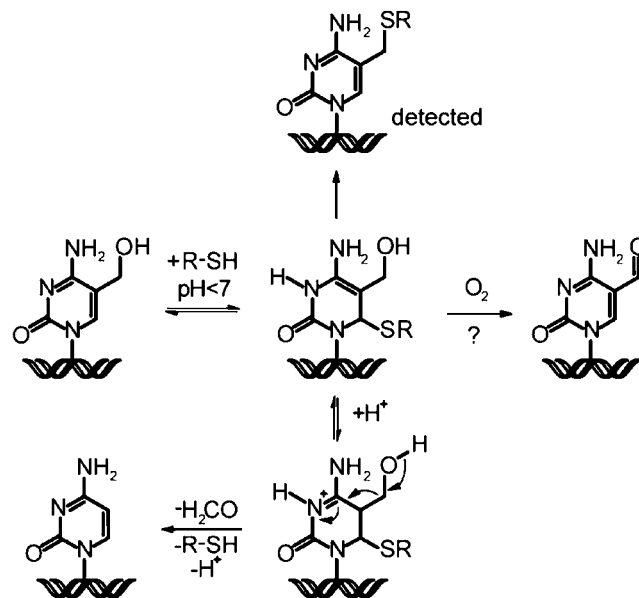
**Figure 2.** Investigation of the oxidation reactions of either hmdC or fdC in a hairpin-oligonucleotide (CpG-ODN 1, 2) with increasing concentration of  $\beta$ -mercaptoethanol/imidazole (pH 5.0, 50 °C, 48 h). Reaction yields (normalized to dT [%]) are plotted against the concentration of  $\beta$ -mercaptoethanol [% v/v]. The yellow data points show the intensity of the mass signal of the thiol adduct 5-((2''-hydroxyethyl)thio)methyl-dC (see top structure of Scheme 3), which was scaled to the right ordinate.

saturation by the thiol has a dramatic influence on the event of oxidation. In the absence of thiols we detected fdC at about 0.2% in ODN1 (48 h, 37 °C, pH 5.0). Other typical pyrimidine oxidation products were not detected regardless of the reaction conditions. We also monitored the levels of the well-established dG oxidation product 8-oxo-dG and noted here no significant level change (Figure 2, black curve), arguing for a thiol-catalyzed oxidation of hmdC to fdC.

Analyzing the mixture by mass spectrometry in more detail revealed the presence of 5-((2''-hydroxyethyl)thio)methyl-dC (Figure 2, yellow curve; top structure in Scheme 3), which shows that a 5-methylene intermediate may be formed during the reaction, which was first described by the Klimasauskas group.<sup>28</sup>

Treatment of ODN2 (fdC) at 80% v/v  $\beta$ -ME gave rise to the formation of the oxidized product cadC, but the reaction is

**Scheme 3.** Depiction of the Thiol-Catalyzed Oxidation of hmdC to fdC and the Proposed Mechanism of the C–C Bond Cleavage of hmdC to dC. R-SH =  $\beta$ -Mercaptoethanol R =  $\text{CH}_2\text{CH}_2\text{OH}$



comparatively slow (Figure 2, green curve). The formation of a dithioacetal of fdC was not detected (see SI). It should be noted that concomitant deformylation of fdC or decarboxylation of the oxidation product cadC to form dC in the presence of  $\beta$ -ME (see last section) may cause a slight underestimation of the oxidation rate.

In summary, experiments on the nucleoside and duplex level reveal that the oxidation of hmdC to fdC is a relatively fast process that is furthermore catalyzed by thiols. This result has to be taken into account when biological samples are investigated regarding the fdC levels.

**Deamination Reactions.** We next incubated the different nucleosides at pH 7.4 in water to investigate the deamination of dC, mdC, hmdC, and fdC to dU, dT, hmdU, and fdU (5-formyl-2'-deoxyuridine), respectively. The data are depicted in Figure 3. Clearly evident is that dC, mdC, hmdC, and fdC are deaminated under these conditions by about the same extent. Deamination of cadC was not detected. To obtain kinetic data at 37 °C, we determined the deamination rate constants at four

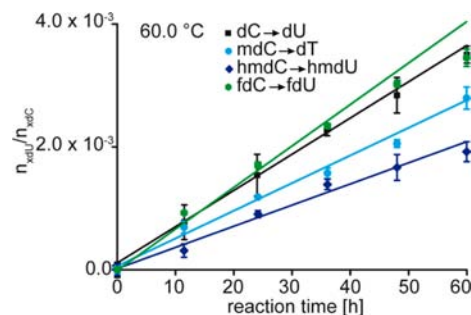


**Figure 3.** Deamination kinetics of dC to dU (black), mdC to dT (cyan), hmdC to hmdU (blue), and fdC to fdU (green) at 60.0 °C, pH 7.4. Depicted are the means of triplicate experiments; error bars reflect the standard deviations. For details of the kinetic measurements at 67.5, 75.0, and 82.5 °C and linear regression analyses see SI.

different temperatures (see SI) and extrapolated the pseudo-first-order deamination rates to 37 °C. The data are compiled in Table 2.

**Table 2. Rate Constants  $k$  and Activation Energies  $E_a$  for the Deamination of dC, mdC, hmdC, and fdC at pH 7.4**

	$k_{37\text{ °C}}$ [ $s^{-1}$ ]	$E_a$ [ $kJ\ mol^{-1}$ ]
dC→dU	$9.4 \pm 0.5 \times 10^{-10}$	$108.7 \pm 1.9$
mdC→dT	$7.8 \pm 0.3 \times 10^{-10}$	$105.0 \pm 2.5$
hmdC→hmdU	$5.8 \pm 0.8 \times 10^{-10}$	$104.8 \pm 3.9$
fdC→fdU	$1.2 \pm 0.2 \times 10^{-9}$	$102.2 \pm 2.4$

At 37 °C, the deamination rates of dC, mdC, hmdC, and fdC to form their corresponding 2'-deoxyuridine derivatives are approximately the same with  $(6-12) \times 10^{-10}\ s^{-1}$  on the nucleoside level. The determined rate constant and activation energy for the deamination of dC are in good agreement with those reported for single-stranded DNA.<sup>29</sup> Bearing in mind that the rates are more than 2 orders of magnitude lower in double-stranded DNA,<sup>29,30</sup> our data argue that spontaneous deamination of hmdC, fdC, and cadC should be a negligible background reaction in comparison to the oxidation of hmdC to form fdC ( $k_{37\text{ °C}} = 1.3 \pm 0.1 \times 10^{-8}\ s^{-1}$ ;  $E_a = 20.8 \pm 2.2\ kJ\ mol^{-1}$ ). If, consequently, significant amounts of deaminated compounds are detected, we conclude that these are likely derived from an enzymatic process.

**C–C bond Cleaving Reactions.** To investigate the reaction of hmdC, fdC, and cadC to form dC we heated the nucleosides for 60 h in water at pH 7.4 at 60 and 80 °C. At 60 °C we detected only traces of dC and the obtained reaction rates at 80 °C were slow (SI, Figure S9 and Table 3), showing that uncatalyzed C–C bond cleavage reactions can be neglected.

This picture changes in the presence of thiols, which we recently reported to catalyze the decarboxylation of cadC.<sup>18</sup> To investigate the conditions of the thiol-mediated decarboxylation reaction in more detail, we treated the cadC-containing ODN3 with increasing concentrations of  $\beta$ -ME for 48 h at different pH-values and different temperatures in the presence of imidazole.<sup>18</sup> The oligonucleotides were isolated and analyzed by LC–MS/MS as outlined in Scheme 2. The results of the experiments are depicted in Figure 4. Clearly evident is that under the investigated conditions (pH 5.0 and 50 °C) decarboxylation of cadC is a relatively efficient reaction. The yield of dC increased along with the concentration of  $\beta$ -ME up to 28%. A lower temperature of 37 °C and a higher pH-value of 7.4 resulted in a strong reduction of the dC yield, which shows that the decarboxylation reaction is an activated proton catalyzed reaction. We next performed analogous experiments with hmdC and fdC (pH 5.0, 50 °C, 48 h). Figure 5 compares the C–C bond cleaving yields of all three nucleosides embedded in the hairpin duplex structures.

We noticed that hmdC dehydroxymethylates to give dC. However, the obtained yield of dC was very small (0.5%). Far higher yields were reported by the Klimasauskas group, who applied a mutated DNA methyltransferase and by the Sowers

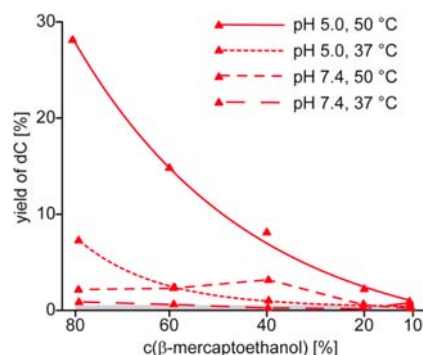


**Figure 4.** Investigation of the C–C bond cleavage reaction of cadC to dC in a hairpin-oligonucleotide (CpG-ODN 3) in a  $\beta$ -mercaptoethanol/imidazole mixture. Depicted are the reaction yields (normalized to dT [%]) depending on the concentration of  $\beta$ -mercaptoethanol [% v/v] at pH = 5.0 or 7.4 and at 37 or 50 °C after 48 h. The gray area reflects the limit of quantification.

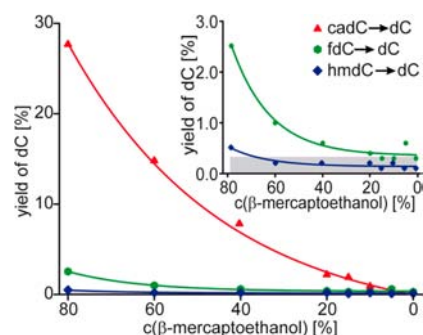


**Figure 5.** Investigation of the C–C bond cleavage reactions of either hmdC, fdC, or cadC in a hairpin-oligonucleotide (CpG-ODN 1, 2, 3) in a  $\beta$ -mercaptoethanol/imidazole mixture (pH 5.0, 50 °C, 48 h). Depicted are the reaction yields (normalized to dT [%]) of hmdC (blue), fdC (green), and cadC (red) to dC depending on the concentration of  $\beta$ -mercaptoethanol [% v/v]. The gray area in the inset shows the limit of quantification.

group, who used photohydration conditions.<sup>16,17,20</sup> For fdC, in contrast, we observed considerable deformylation and obtained yields of up to 2.5%. Decarboxylation of cadC is most efficient with an obtained yield of up to 28%.

We next studied how different sequences would affect the C–C bond cleaving and deamination reactions and repeated the experiments with ODNs 4–6 which feature the xdc-derivatives in a non-CpG context (Figure 6). We observed only a small reactivity difference in these sequences compared to the CpG-ODNs. The yields of deamination products were found to be lower than 0.4% under these conditions.

The data show that both fdC and cadC can undergo C–C bond cleavage reactions mediated by thiols. Dehydroxymethylation of hmdC is in contrast a considerably slower process.

To gain deeper insights into the thiol catalysis of the C–C bond cleavage reactions, we finally computed the reaction energies using quantum-chemical methods. Computational details are described in the SI. Carboxylated nucleobases (caC and caU) were capped at the N1 position with a methyl

**Table 3. Rate Constants for the Non-Thiol-Mediated C–C Bond Cleavage of hmdC, fdC, and cadC to dC at pH 7.4 at 80 °C**

	hmdC→dC	fdC→dC	cadC→dC
$k_{80\text{ °C}}$ [ $s^{-1}$ ]	$1.3 \pm 0.2 \times 10^{-9}$	$7.3 \pm 1.1 \times 10^{-9}$	$6.9 \pm 0.7 \times 10^{-9}$

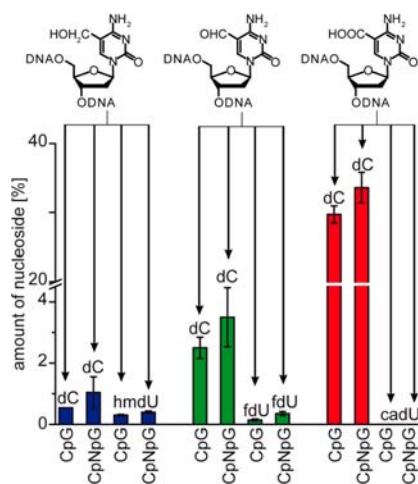


**Figure 6.** The C–C-bond cleavage of hmdC, fdC, and cadC to dC is almost independent of the sequence context. Investigation of the C–C bond cleavage and deamination reactions of either hmdC, fdC, or cadC in a hairpin-oligonucleotide (CpG-ODN 1, 2, 3; CpNpG-ODN 4, 5, 6) in a 80% (v/v)  $\beta$ -mercaptoethanol/imidazole mixture (pH 5.0, 50 °C, 48 h). Depicted are the reaction yields (normalized to dT [%]) of hmdC (blue), fdC (green), and cadC (red) to dC as well as the corresponding deamination products hmdU and fdU. Depicted are the means of triplicate experiments; error bars reflect the standard deviations.

group. To describe the explicit solvent–solute hydrogen bonds, five water molecules were included in the study. Ideally, one would like to describe more of the long-range electrostatic solute–solvent interactions by including more water molecules in the calculations. This would, however, mean a computational effort which is beyond the scope of this work. A crude way to approximate the influence of the continuum is to use an implicit solvent model. Here, we have performed calculations with an implicit solvent cavity using the COSMO-model<sup>31</sup> (data shown in SI). Although the energetics are clearly affected, the overall trend remains the same. Triple-zeta basis sets<sup>32</sup> were used throughout the calculations. RI-MP2<sup>32,33</sup> reaction energies, obtained using the DFT/B3LYP-D3<sup>34–36</sup> energy optimized structures, are depicted in Figure 7. No transition state search was carried out as the reaction rates are already obtained from the experimental data presented above.

We first computed the direct decarboxylation of isoorotate (caU), a reaction that is catalyzed by the enzyme isoorotate decarboxylase (IDCase).<sup>37,38</sup> We assumed in our study a direct decarboxylation via formation of a vinyl anion type intermediate. Similar mechanistic ideas were the basis of a recent detailed mechanistic and structural study of the IDCase.<sup>39</sup> We obtained by our calculations a rather high energy of +34 kcal mol<sup>-1</sup> for the vinyl anion of U (gray intermediate in Figure 7). In agreement with our results from the thiol-free reaction conditions, our data show that a direct decarboxylation mechanism for caC is unlikely. In comparison to the vinyl anion of U, the energy of the vinyl anion of C is with +47 kcal mol<sup>-1</sup> significantly higher. This may in part explain the observed weak activity<sup>39</sup> of IDCase to decarboxylate ScaC to C. In contrast, the energetics of the thiol addition at the C6 position of caC and the subsequent decarboxylation are much more favorable: Calculations predict an only slightly endothermic reaction energy of +6 kcal mol<sup>-1</sup> for the decarboxylation of the thiol-reacted anionic intermediate. Overall, the reaction of the C6 position with the thiol reduces

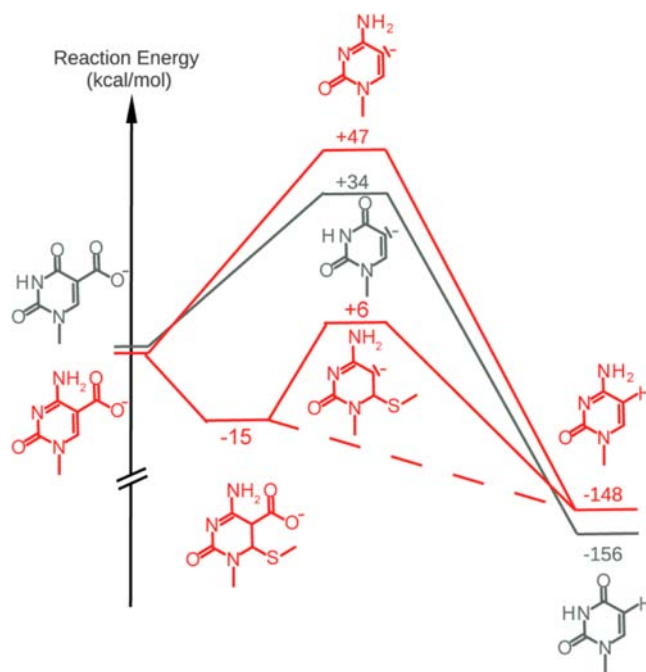


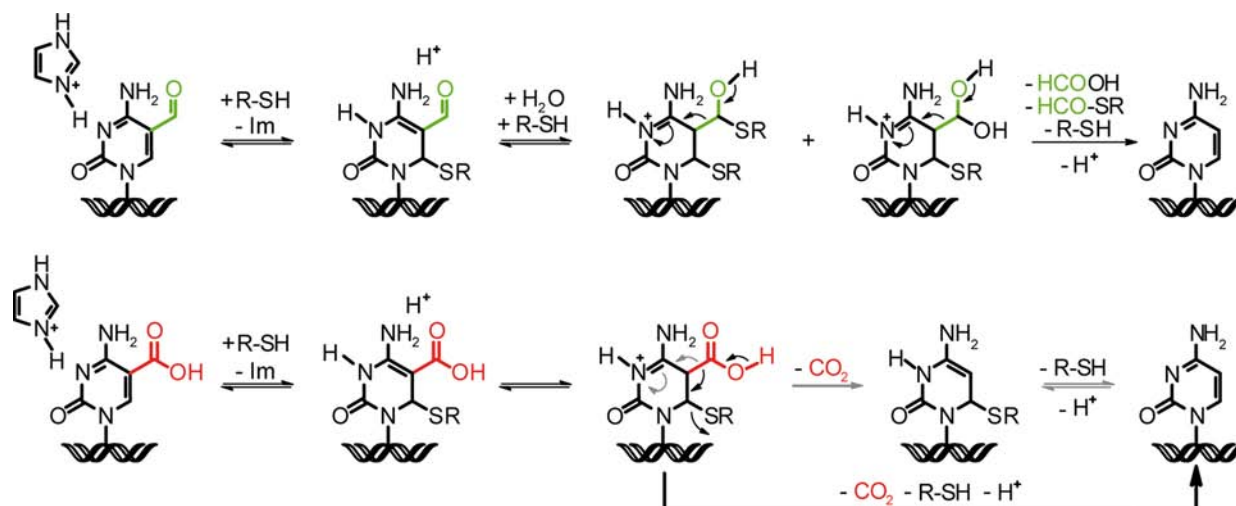
**Figure 7.** Schematic representation of different decarboxylation pathways. Depicted are the reaction energies obtained from quantum chemical calculations.

the energy of the corresponding anionic intermediate by more than 40 kcal mol<sup>-1</sup> (Figure 7, intermediates shown in red). This explains why the reaction of cadC with a thiol leads to fast decarboxylation. We also noted during the computational study that simultaneous decarboxylation and thiol elimination is an even more favorable process. This reaction pathway is symbolized with dotted lines in Figure 7 and illustrated in Scheme 4. In summary, the calculations support the influence of the thiol catalysis.

## CONCLUSIONS

We show that the new nucleosides hmdC, fdC, and cadC possess an increased reactivity compared to mdC and dC. First, the intrinsic deamination rates of hmdC and fdC are comparable to those of mdC and dC. Second, hmdC is more susceptible to oxidation. It reacts surprisingly quickly to fdC if exposed to atmospheric oxygen, which is a problem that needs to be considered when DNA is isolated from biological material for the determination of fdC. In addition, the reaction of hmdC to fdC is accelerated in the presence of thiols. If fdC is exposed to atmospheric oxygen further oxidation to cadC is a rather inefficient process.

Third and importantly, fdC and cadC can undergo thiol-mediated and acid-catalyzed C–C bond cleavage reactions to form dC under release of formic acid and CO<sub>2</sub>, respectively (see Scheme 4). Here decarboxylation is by a factor of 11 more efficient than the deformylation of fdC. If we consider that DNA demethylation requires stepwise oxidation of hmdC to fdC and cadC, both deformylation of fdC and decarboxylation of cadC could take place via alternative active demethylation mechanisms.

Scheme 4. Proposed Mechanisms of the Thiol-Mediated and Acid-Catalyzed C–C Bond Cleavage Reactions of fdC and cadC to dC<sup>a</sup>

<sup>a</sup>The reactions are thought to proceed via a covalent enamine intermediate. The deformylation reaction of fdC further requires the addition of a nucleophile (water or thiol) to the aldehyde before the release of formic acid (or the thiol ester) can proceed. In principal, the release of formic acid from fdC or carbon dioxide from cadC and thiol elimination could occur simultaneously or in two steps (shown by gray or black arrows, respectively). R-SH =  $\beta$ -mercaptoethanol; Im = imidazole.

## ■ ASSOCIATED CONTENT

### Supporting Information

Experimental procedures and spectroscopic data of standards for the UHPLC-MS/MS analysis, detailed procedures for mass spectrometric measurements, and method development. This material is available free of charge via the Internet at <http://pubs.acs.org>.

## ■ AUTHOR INFORMATION

### Corresponding Author

Thomas.Carell@cup.uni-muenchen.de

### Author Contributions

<sup>†</sup>S.S. and T.P. contributed equally.

### Notes

The authors declare no competing financial interest.

## ■ ACKNOWLEDGMENTS

This work was supported by the Deutsche Forschungsgemeinschaft via SFB749 (TPA4/C7) and the Excellence cluster EXC114 (CiPS<sup>M</sup>). S.S., T.P., and A.S.S. thank the Fonds der Chemischen Industrie for predoctoral fellowships. K.S. and C.O. thank Dr. Denis Flaig for helpful discussions. G.K. thanks the Japan Society for the Promotion of Science (JSPS) as a JSPS Postdoctoral Fellow for Research Abroad.

## ■ REFERENCES

- (1) Kriaucionis, S.; Heintz, N. *Science* **2009**, *324*, 929.
- (2) Tahiliani, M.; Koh, K. P.; Shen, Y.; Pastor, W. A.; Bandukwala, H.; Brudno, Y.; Agarwal, S.; Iyer, L. M.; Liu, D. R.; Aravind, L.; Rao, A. *Science* **2009**, *324*, 930.
- (3) Pfaffeneder, T.; Hackner, B.; Truß, M.; Münzel, M.; Müller, M.; Deiml, C. A.; Hagemeyer, C.; Carell, T. *Angew. Chem., Int. Ed.* **2011**, *50*, 7008.
- (4) He, Y.-F.; Li, B.-Z.; Li, Z.; Liu, P.; Wang, Y.; Tang, Q.; Ding, J.; Jia, Y.; Chen, Z.; Li, L.; Sun, Y.; Li, X.; Dai, Q.; Song, C.-X.; Zhang, K.; He, C.; Xu, G.-L. *Science* **2011**, *333*, 1303.
- (5) Ito, S.; Shen, L.; Dai, Q.; Wu, S. C.; Collins, L. B.; Swenberg, J. A.; He, C.; Zhang, Y. *Science* **2011**, *333*, 1300.

(6) Guo, J. U.; Su, Y.; Zhong, C.; Ming, G.-L.; Song, H. *Cell* **2011**, *145*, 423.

(7) Cortellino, S.; Xu, J.; Sannai, M.; Moore, R.; Caretti, E.; Cigliano, A.; Le Coz, M.; Devarajan, K.; Wessels, A.; Soprano, D.; Abramowitz, L. K.; Bartolomei, M. S.; Rambow, F.; Bassi, M. R.; Bruno, T.; Fanciulli, M.; Renner, C.; Klein-Szanto, A. J.; Matsumoto, Y.; Kobi, D.; Davidson, I.; Alberti, C.; Larue, L.; Bellacosa, A. *Cell* **2011**, *146*, 67.

(8) Nabel, S. N.; Jia, H.; Ye, Y.; Shen, L.; Goldschmidt, H. L.; Stivers, J. T.; Zhang, Y.; Kohli, R. M. *Nat. Chem. Biol.* **2012**, *8*, 751.

(9) Bienvenu, C.; Wagner, J. R.; Cadet, J. *J. Am. Chem. Soc.* **1996**, *118*, 11406.

(10) Cao, H.; Wang, Y. *Nucleic Acids Res.* **2007**, *35*, 4833.

(11) Wagner, J. R.; Cadet, J. *Acc. Chem. Res.* **2010**, *43*, 564.

(12) Liu, S.; Wang, J.; Su, Y.; Guerrero, C.; Zeng, Y.; Mitra, D.; Brooks, P. J.; Fisher, D. E.; Song, H.; Wang, Y. *Nucleic Acids Res.* **2013**, *41*, 6421.

(13) Taghizadeh, K.; McFaline, J. L.; Pang, B.; Sullivan, M.; Dong, M.; Plummer, E.; Dedon, P. C. *Nat. Protoc.* **2008**, *3*, 1287.

(14) Ravanat, J.-L.; Douki, T.; Duez, P.; Gremaud, E.; Herbert, K.; Hofer, T.; Lasserre, L.; Saint-Pierre, C.; Favier, A.; Cadet, J. *Carcinogenesis* **2002**, *23*, 1911.

(15) Globisch, D.; Münzel, M.; Müller, M.; Michalak, S.; Wagner, M.; Koch, S.; Brückl, T.; Biel, M.; Carell, T. *PLoS One* **2010**, *5*, e15367 DOI: 10.1371/journal.pone.0015367.

(16) Hamm, S.; Just, G.; Lacoste, N.; Moitessier, N.; Szyf, M.; Mamer, O. *Bioorg. Med. Chem. Lett.* **2008**, *18*, 1046.

(17) Liutkeviciute, Z.; Lukinavicius, G.; Masevicius, V.; Daujotyte, D.; Klimasauskas, S. *Nat. Chem. Biol.* **2009**, *5*, 400.

(18) Schiesser, S.; Hackner, B.; Pfaffeneder, T.; Müller, M.; Hagemeyer, C.; Truss, M.; Carell, T. *Angew. Chem., Int. Ed.* **2012**, *51*, 6516.

(19) Wu, S. C.; Zhang, Y. *Nat. Rev. Mol. Cell Biol.* **2010**, *11*, 607.

(20) Privat, E.; Sowers, L. C. *Chem. Res. Toxicol.* **1996**, *9*, 745.

(21) Tardy-Planechaud, S.; Fujimoto, J.; Lin, S. S.; Sowers, L. C. *Nucleic Acids Res.* **1997**, *25*, 553.

(22) Dai, Q.; He, C. *Org. Lett.* **2011**, *13*, 3446.

(23) Münzel, M.; Lischke, U.; Stathis, D.; Pfaffeneder, T.; Gnerlich, F. A.; Deiml, C. A.; Koch, S. C.; Karaghiosoff, K.; Carell, T. *Chem.—Eur. J.* **2011**, *17*, 13782.

(24) Steigenberger, B.; Schiesser, S.; Hackner, B.; Brandmayr, C.; Laube, S. K.; Steinbacher, J.; Pfaffeneder, T.; Carell, T. *Org. Lett.* **2013**, *15*, 366.

(25) Münzel, M.; Globisch, D.; Trindler, C.; Carell, T. *Org. Lett.* **2010**, *12*, 5671.

(26) Münzel, M.; Globisch, D.; Brückl, T.; Wagner, M.; Welzmler, V.; Michalakis, S.; Müller, M.; Biel, M.; Carell, T. *Angew. Chem., Int. Ed.* **2010**, *49*, 5375.

(27) Spruijt, Cornelia G.; Gnerlich, F.; Smits, Arne H.; Pfaffeneder, T.; Jansen, Pascal W. T. C.; Bauer, C.; Münzel, M.; Wagner, M.; Müller, M.; Khan, F.; Eberl, H. C.; Mensinga, A.; Brinkman, Arie B.; Lephikov, K.; Müller, U.; Walter, J.; Boelens, R.; van Ingen, H.; Leonhardt, H.; Carell, T.; Vermeulen, M. *Cell* **2013**, *152*, 1146.

(28) Liutkevičiūtė, Z.; Kriukienė, E.; Grigaitytė, I.; Masevičius, V.; Klimašauskas, S. *Angew. Chem., Int. Ed.* **2011**, *123*, 2138.

(29) Frederico, L. A.; Kunkel, T. A.; Shaw, B. R. *Biochemistry* **1990**, *29*, 2532.

(30) Shen, J.-C.; Rideout, W. M., III; Jones, P. A. *Nucleic Acids Res.* **1994**, *22*, 972.

(31) Klamt, A.; Schüürmann, G. *J. Chem. Soc., Perkin Trans. 2* **1993**, *5*, 799.

(32) Weigend, F.; Häser, M.; Patzelt, H.; Ahlrichs, R. *Chem. Phys. Lett.* **1998**, *294*, 143.

(33) Feyereisen, M.; Fitzgerald, G.; Komornicki, A. *Chem. Phys. Lett.* **1993**, *208*, 359.

(34) Lee, C.; Yang, W.; Parr, R. G. *Phys. Rev. B* **1998**, *37*, 785.

(35) Becke, A. D. *J. Chem. Phys.* **1993**, *98*, 5648.

(36) Grimme, S.; Ehrlich, S.; Goerigk, L. *J. Comput. Chem.* **2011**, *32*, 1456.

(37) Smiley, J. A.; Angelot, J. M.; Cannon, R. C.; Marshall, E. M.; Asch, D. K. *Anal. Biochem.* **1999**, *266*, 85.

(38) Palmatier, R. D.; McCroskey, R. P.; Abbott, M. T. *J. Biol. Chem.* **1970**, *245*, 6706.

(39) Xu, S.; Li, W.; Zhu, J.; Wang, R.; Li, Z.; Xu, G.-L.; Ding, J. *Cell Res.* **2013**, DOI: 10.1038/cr.2013.107.